Preparation of highly active AlSBA-15-supported platinum catalyst for thiophene hydrodesulfurization

doi: info:doi/10.1016/j.apcatb.2007.07.012

Preparation of highly active AlSBA-15-supported platinum catalyst for thiophene hydrodesulfurization

doi: info:doi/10.1016/j.apcatb.2007.07.012

Applied Catalysis B: Environmental

Full Length Article

Revised

Preparation of highly active AlSBA-15-supported platinum catalyst for thiophene hydrodesulfurization

Yasuharu Kanda[a,*], Tomohiro Aizawa[a], Takao Kobayashi[a], Yoshio Uemichi[a], Seitaro Namba[b] and Masatoshi Sugioka[a]

[a]Department of Applied Chemistry, Muroran Institute of Technology, 27-1 Mizumoto-cho, Muroran 050-8585, Japan

[b]Department of Materials, Teikyo University of Science and Technology, 2525 Yatsusawa, Uenohara, Yamanashi 409-0193, Japan

* Corresponding author. Tel.: +81 143 46 5750; fax: +81 143 46 5750.

E-mail address: kanda@mmm.muroran-it.ac.jp (Y. Kanda),

msugioka@mmm.muroran-it.ac.jp (M. Sugioka).

Abstract

The catalytic activities of various noble metals (Pt, Pd, Rh, and Ru) supported on siliceous SBA-15 and Al-containing SBA-15 (AlSBA-15) for hydrodesulfurization (HDS) of thiophene at 350 °C were investigated. AlSBA-15 was prepared by a grafting method using aluminum isopropoxide ($Al(OC_3H_7)_3$) hexane solution. The HDS activity of Pt/AlSBA-15 catalyst was the highest among those of various supported noble metal catalysts, and this activity was higher than that of commercial $CoMo/Al_2O_3$ HDS catalyst. The catalysts were characterized by XRD analysis, hydrogen adsorption, 2-propanol dehydration, cumene cracking, and FT-IR. Dispersion of Pt on SBA-15 was remarkably enhanced by Al grafting. It was revealed that the acidity of AlSBA-15 was higher than that of SBA-15. Furthermore, Brønsted acid sites were observed on AlSBA-15. FT-IR spectra of thiophene adsorbed on AlSBA-15 indicate that thiophene molecules interact with Brønsted acid sites on the surface of AlSBA-15 and that the strength of this interaction was stronger than that of SBA-15. Based on these results, thiophene molecules activated on Brønsted acid site of AlSBA-15 and hydrogen molecules activate to form spillover hydrogen on Pt particles in Pt/AlSBA-15 catalyst in the HDS of thiophene.

Keywords

Acid rain prevention; Hydrodesulfurization; Thiophene; SBA-15; Noble metal catalyst

1. Introduction

The damage to nature and environment by acid rain on a global scale is a serious problem. Sulfur oxides (SO_x) are produced by combustion of organic sulfur compounds in petroleum and coal used for boilers and engines of power plants and cars. Hydrodesulfurization (HDS) of petroleum feedstock is an important process in the petroleum industry to produce clean fuels [1–4]. However, recently, the development of highly active HDS catalysts, which exhibit higher activity

than commercial $CoMo/Al_2O_3$ HDS catalysts, have been claimed in the petroleum industry to produce fuels with lower sulfur content [5,6]. It has been accepted that noble metal catalysts are potentially new HDS catalysts for petroleum [7–12]. The authors have also investigated the development of highly active noble metal HDS catalysts supported on zeolites [13–15,22].

Recently, mesoporous silicates such as FSM-16, MCM-41, and SBA-15, which have larger pore diameters and higher surface areas than zeolites, have attracted wide attention as new materials for catalysts and catalyst supports. Some attempts have been made to develop new HDS catalysts based on mesoporous silicates [16–19]. In previous papers, we have reported that noble metals, especially platinum, supported on mesoporous silicates such as FSM-16 [20] and MCM-41 [21,22], showed high activity in the HDS of thiophene, and noble metals supported on mesoporous silicates can potentially be used as new HDS catalysts for petroleum feedstock. Furthermore, the catalytic activity of Pt/MCM-41 for the HDS of thiophene was enhanced by Al-modification of the MCM-41 surface and Brønsted acid sites in Pt/Al-modified MCM-41 catalyst play an important role in the HDS of thiophene [23,24]. Generally, the Brønsted acid site of mesoporous silicate is generated by incorporation of Al atoms into the silicate framework. Mesoporous silica SBA-15, which has a larger pore diameter than MCM-41, can be synthesized using triblock copolymer and strong acidic media. However, because the Al source dissolves in strong acidic media when used in the synthesis of SBA-15, direct incorporation of Al atoms into the framework of SBA-15 is not efficient. Thus, it is expected that the catalytic activity of Pt/SBA-15 for HDS reaction is enhanced by alumination of siliceous SBA-15 support using aluminum isopropoxide.

In the present work, we examined the catalytic performance of noble metals supported on SBA-15 and AlSBA-15 for the HDS of thiophene to develop highly active mesoporous silicate catalyst for HDS of petroleum feedstock. Furthermore, we studied the reaction mechanism in the HDS of thiophene over highly active Pt/AlSBA-15 catalyst.

2. Experimental

2. 1. Preparation of catalysts

Siliceous SBA-15 was prepared by conventional hydrothermal process, described earlier [38, 39] using tetraethoxysilane ($Si(OC_2H_5)_4$, Aldrich Chemical Co.), triblock copolymer (poly(ethylene glycol)$_{20}$-poly(propylene glycol)$_{70}$-poly(ethylene glycol)$_{20}$, Dai-ichi Kogyo Seiyaku), and hydrogen chloride (HCl, Kanto Chemical Co.). The solid product was washed by water followed by drying at 100 °C and calcination in air at 557 °C for 8 h. AlSBA-15 (Si/Al = 15) was prepared by a grafting method using aluminum isopropoxide ($Al(OC_3H_7)_3$, Kanto Chemical Co.) dry hexane solution at room temperature for 24 h. The obtained sample was washed by dry hexane and was calcined at 400 °C for 2 h. Addition of sodium to AlSBA-15 support was also performed by an impregnation method using sodium hydroxide (NaOH, Wako Pure Chemical Industries) aqueous solution. After sodium impregnation, Na-added AlSBA-15 (Na-AlSBA-15) was dried at 120 °C and was calcined at 500 °C for 4 h. Supported noble metal catalysts were also prepared by an impregnation method using noble metal chloride (H_2PtCl_6•$6H_2O$, $PdCl_2$, $RhCl_3$•$3H_2O$, $RuCl_3$•$3H_2O$, Kanto Chemical Co.) aqueous solution; the amount of noble metal loading was 5 wt%. $PdCl_2$ was dissolved in 1.0 mol l^{-1} HCl aqueous solution because $PdCl_2$ did not dissolve completely in water. After impregnation, the samples were dried at 120 °C followed by calcination at 500 °C for 4 h. The supported noble metal catalysts were treated by helium stream at 500 °C for 1 h and were reduced by hydrogen at 450 °C for 1 h before the reaction.

2. 2. Hydrodesulfurization of thiophene

HDS of thiophene was performed at 350 °C under 0.1 MPa by a conventional fixed-bed flow reactor. Thiophene was introduced into the reactor by passing hydrogen (30 ml min^{-1}) through a thiophene trap cooled at 0 °C. Reaction conditions were as follows: catalyst weight = 0.1 g, H_2/thiophene = 30 mol mol^{-1}, W/F = 37.9 g h mol^{-1}. The reaction products were analyzed by gas

chromatograph (FID) equipped with silicone DC-550 (2 m, 150 °C) and VZ-7 (4 m, 0 °C) columns, respectively. We used $CoMo/Al_2O_3$ (Nippon Cyanamid Co.) as a reference catalyst.

2. 3. Characterization of catalysts

2. 3. 1. Nitrogen adsorption isotherm

The nitrogen adsorption isotherm at −196 °C was measured by using Micromeritics ASAP 2000. The specific surface areas of SBA-15 and AlSBA-15 were calculated by the BET method and the pore size distributions by the BJH method.

2. 3. 2. Dispersion of platinum

The dispersion of platinum on SBA-15 and AlSBA-15 was measured by XRD and hydrogen adsorption. XRD was performed using a Rigaku diffract meter with Cu Kα radiation. Adsorption of hydrogen on the supported Pt catalyst was performed using a glass vacuum system at 25 °C. The supported Pt catalysts were evacuated at 500 °C for 1 h followed by reduction with hydrogen (26.7 kPa) at 450 °C for 1 h and evacuation at the same temperature for 1 h before hydrogen adsorption.

2. 3. 3. Acidities of SBA-15 and AlSBA-15

The acidities of SBA-15 and AlSBA-15 were evaluated by 2-propanol (2-PA) dehydration (200 °C) and cumene cracking (400 °C) using a pulse reactor with helium carrier gas. In both reactions, catalysts (0.03 g) were charged into the reactor and were pretreated at 500 °C for 1 h before the reaction. 2-PA or cumene (0.2 μl) was introduced into the reactor using a micro syringe. The reaction products of 2-PA dehydration and cumene cracking were separated using a silicone DC-550 (2 m, 130 °C) column and a PEG-1000 column (2 m, 80 °C), respectively. However, the reaction products of 2-PA dehydration were trapped by liquid nitrogen and were flashed by boiling water before the separation. After the separation, the reactant and products were analyzed by thermal conductivity detector (TCD).

2. 3. 4. Measurement of FT-IR spectra

FT-IR spectra of pyridine and thiophene adsorbed on SBA-15 and AlSBA-15 were observed using a Jasco FT-IR spectrometer. The catalysts were evacuated at 500 °C for 2 h before the measurement.

3. Results and Discussion

3. 1. Textural properties of SBA-15 and AlSBA-15

The textural properties of SBA-15 and AlSBA-15 were characterized by XRD and nitrogen adsorption. In the XRD pattern of SBA-15, an intense peak at 0.92° and low-intensity peaks at 1.64° and 1.90°, which were attributed to a hexagonal structure, were observed (Fig. 1). After Al grafting, the XRD pattern of AlSBA-15 was the same as that of siliceous SBA-15. Fig. 2 shows the nitrogen adsorption isotherms of SBA-15 and AlSBA-15. SBA-15 shows that the amount of nitrogen adsorption sharply increased in the range of relative pressure from 0.7 to 0.75. This result was ascribed to capillary condensation, which is characteristic of ordered mesoporous material. Furthermore, the shape of the adsorption isotherm of AlSBA-15 was similar to that of SBA-15. These results indicate that uniform pore structure of SBA-15 was maintained even after Al grafting. Textural properties were calculated by the nitrogen adsorption isotherm (Table 1). SBA-15 showed high surface area (847 $m^2 g^{-1}$) and pore volume (1.12 $cm^3 g^{-1}$) but these properties were decreased by Al grafting. However, these properties of AlSBA-15 remained high even after Al grafting. Fig. 3 shows the pore size distribution of SBA-15 and AlSBA-15 calculated by the BJH method. The pore size distribution of SBA-15 was shifted to more pores of smaller diameters by Al grafting. This result suggests that Al atoms exist in the inside pore of SBA-15.

3. 2. Catalytic activities of noble metals supported on SBA-15 and AlSBA-15

We examined the catalytic activities of noble metals supported on SBA-15 for the HDS of thiophene at 350 °C. It was revealed that the catalytic activities of noble metals supported on SBA-l5

varied remarkably with the type of noble metals (Fig. 4). The order of the activities of these catalysts after reaction for 2 h was Pt/SBA-15 > Pd/SBA-15 > Rh/SBA-15 > Ru/SBA-l5. The activity of Pt/SBA-15 catalyst was similar to that of presulfided $CoMo/Al_2O_3$ HDS catalyst.

In a previous paper, we reported that the catalytic activity of Pt supported on siliceous MCM-41 for HDS of thiophene was enhanced by Al modification of MCM-41 surface [24]. Thus, it was expected that the HDS activity of noble metal supported on SBA-15 was also enhanced by Al modification. We examined the catalytic activities of noble metals supported on AlSBA-15 for the HDS of thiophene at 350 °C in order to develop much more highly active SBA-l5-based HDS catalysts. Pt/AlSBA-15 catalyst showed the highest activity among noble metal/AlSBA-15 catalysts, and this activity was higher than that of presulfided $CoMo/Al_2O_3$ HDS catalyst (Fig. 5).

Fig. 6 shows the comparison of HDS activities of supported Pt catalysts. The HZSM-5 zeolite-supported Pt catalyst showed the highest HDS activity among supported Pt catalysts. However, reaction products in the HDS of thiophene over Pt/HZSM-5 catalyst were cracked by strong Brønsted acidity of HZSM-5 [15]. The HDS activity of Pt/Al_2O_3-modified MCM-41 (Al_2O_3-MCM-41) catalyst was equivalent to that of Pt/HZSM-5. In contrast to Pt/HZSM-5, the reaction product was mainly C_4 hydrocarbons in the HDS of thiophene over Pt/Al_2O_3-MCM-41 catalyst [23,24]. Since cracking of hydrocarbons by strong acidity of zeolite is not favorable for producing gasoline and diesel fuel, Pt/Al_2O_3-MCM-41 is superior to Pt/HZSM-5 as a HDS catalyst. The HDS activity of Pt/AlSBA-15 catalyst was lower than that of Pt/Al_2O_3-MCM-41 catalyst. On the other hand, AlSBA-15 has a larger pore diameter (7.0 nm) compared with Al_2O_3-MCM-41 (2.6 nm). It can be expected that Pt/AlSBA-15 catalyst shows high activity for HDS of bulky organic sulfur compounds. Therefore, Pt/AlSBA-15 catalyst was investigated in detail to understand the causes of the high activity of Pt/AlSBA-15 for the HDS of thiophene.

3. 3. Dispersion of Pt on SBA-15 and AlSBA-15

Fig. 7 shows the XRD patterns of Pt/SBA-15 and Pt/AlSBA-15 catalysts before reduction. The peak height of Pt on SBA-15 was significant, but it decreased on AlSBA-15 compared with SBA-15. This indicates that the dispersion of Pt on AlSBA-15 was higher than that on SBA-15. Table 2 shows the dispersion and particle size of Pt on SBA-15 and AlSBA-15 measured by the hydrogen adsorption method. The particle size of Pt (d_{Pt}, assumed as spherical shape) was calculated by dispersion of Pt, according to the equation $d_{Pt} = 0.944/D$ (D = dispersion of Pt). It was also revealed that Pt dispersion on AlSBA-15 was higher and the particle size was lower than on SBA-15. However, the particle size of Pt on SBA-15 calculated by the Scherrer equation was 14.4 nm; this size was remarkably larger than that calculated by hydrogen adsorption. An explanation of these results is that XRD analysis detects only large Pt particles as the sharp peaks, but the hydrogen adsorption method evaluates the average particle size of Pt.

It was reported that Cl^- ligands in $[PtCl_6]^{2-}$ exchange with the hydroxyl groups on the alumina surface [25,26]. Furthermore, $[PtCl_6]^{2-}$ is adsorbed irreversibly on the alumina surface by drying at 90 °C [26]. In contrast, the hydroxyl group on the silica surface (Si-OH) also acts as a ligand of Pt complex, but Si-OH ligand in Pt complex exchanged reversibly with H_2O even after drying at 90 °C [27]. These results indicate that the interaction between Pt particles and the Al-modified silica surface is stronger than that of the silica surface. Therefore, the dispersion of Pt was significantly enhanced by Al grafting of SBA-15.

3. 4. Acidic properties of SBA-15 and AlSBA-15

We evaluated the acidic properties of SBA-15 and AlSBA-15 based on 2-PA dehydration (200 °C) and cumene cracking (400 °C) reactions using a pulse reactor. It was revealed that SBA-15 showed very low activity for both acid-catalyzed reactions, but AlSBA-15 exhibited remarkably high activity for both acid-catalyzed reactions (Fig. 8). These results indicate that the acidity of AlSBA-15 was remarkably higher than that of SBA-15. We confirmed the existence of the Brønsted acid sites on

AlSBA-15 by the observation of FT-IR spectra of pyridine adsorbed on AlSBA-l5 (l547 cm^{-1}) (Fig. 9).

3. 5. Mechanism of HDS of thiophene on Pt/AlSBA-15 catalyst

Pt/AlSBA-15 catalyst showed higher activity for the HDS of thiophene than Pt/SBA-l5 and commercial $CoMo/Al_2O_3$ catalysts. Thus, we studied the reaction mechanism in the HDS of thiophene over Pt/AlSBA-15 catalyst.

We have reported in previous papers [13–15,20–24,28] that Brønsted acid sites on the supports of noble metal catalysts act as active sites for activation of thiophene. Thus, we supposed that the Brønsted acid site of AlSBA-l5 acts as an active site for the activation of thiophene in the HDS of thiophene. The role of Brønsted acid sites in the HDS reaction was examined by the addition of sodium to highly active Pt/AlSBA-15 catalyst. Table 3 shows the effect of this sodium addition on catalytic activity for thiophene HDS and the properties of Pt/AlSBA-15. The dispersion of Pt was hardly changed by the addition of sodium (except 4 wt% Na loading). However, the HDS activity of the Pt/AlSBA-15 catalyst and Brønsted acidity of the AlSBA-15 support decreased with increasing sodium addition. These results indicate that Brønsted acid sites in supported Pt catalyst participate in the HDS of thiophene.

Furthermore, we observed the FT-IR spectra of thiophene adsorbed on SAB-15 and AlSBA-15 in order to clarify the interaction between silanol groups and thiophene molecules. In the background spectra of SBA-15 evacuated at 500 °C for 2 h, the silanol group was observed at 3745 cm^{-1} (spectrum (i) in Fig. 10 (a)). After introduction of 2 kPa of thiophene onto the SBA-15, the absorption band of Si-OH at 3745 cm^{-1} decreased considerably and a large and broad peak appeared at around 3600 cm^{-1}, which is assigned to the silanol groups interacting with the thiophene molecules (spectrum (ii) in Fig. 10 (a)). However, the decreased absorbance of silanol

groups was completely regenerated by the evacuation at 25 °C, without any shoulder peak at around 3600 cm^{-1} (spectrum (iii) in Fig. 10 (a)).

In the background spectra of AlSBA-15 evacuated at 500 °C for 2 h, the silanol group was observed at 3745 cm^{-1} (spectrum (i) in Fig. 10 (b)). Following the introduction of 2 kPa of thiophene onto the AlSBA-15, the absorption band at 3745 cm^{-1} decreased and shifted to 3606 cm^{-1} (spectrum (ii) in Fig. 10 (b)). The decreased absorbance of the silanol group was almost regenerated by the evacuation at 25 °C, but a slight shoulder peak at 3606 cm^{-1} was observed (spectrum (iii) in Fig. 10 (b)). Furthermore, Fig. 10 (c) and (d) show the FT-IR spectra of thiophene adsorbed on Na-AlSBA-15. The intensity of the band at 3745 cm^{-1} was decreased by increasing sodium addition. In the spectra of Na-AlSBA-15, the absorbance of the silanol groups was also decreased by thiophene introduction. However, the shoulder peak at around 3600 cm^{-1} was not observed after evacuation at 25 °C (spectra (iii) in Fig. 10 (c) and (d)). These results indicate that the interaction between AlSBA-15 with Brønsted acid sites and thiophene is stronger than those of SBA-15 and Na-AlSBA-15 without Brønsted acid sites.

Some modes of coordinated thiophene in organometallic complexes have been reported [29] and two adsorption types of thiophene on catalyst surfaces were proposed [30–32]; (i) via π electrons in aromatic rings and (ii) via sulfur atoms. It was reported that the sulfur atom in thiophene directly interacts with the Brønsted acid site on HY zeolite [32]. According to the theoretical results, the sulfur atom in thiophenes interacts with hydroxyl groups of zeolites [33,34]. Furthermore, the shift in frequency of the silanol group was because of the interaction between the sulfur atom in thiophene and hydroxyl groups of zeolite, and these experimental results were consistent with theoretical results [33]. We also observed that frequency shifts of the silanol group on SBA-15 and AlSBA-15 occurred by thiophene introduction (Fig. 10 (a) and (b)). Thus, thiophene molecules may adsorb on Brønsted acid sites of AlSBA-15 via sulfur atoms. These results confirmed that thiophene is adsorbed and activated on Brønsted acid sites on AlSBA-15 in the HDS of thiophene over Pt/AlSBA-15 catalyst.

We examined the effect of Pt loading on HDS activity of Pt/AlSBA-15 catalyst. The HDS activity of Pt/AlSBA-15 catalyst remarkably enhanced with increasing Pt loading (Fig. 11). However, when Pt loading increased by more than 5 wt%, the HDS activity of Pt/AlSBA-15 catalyst did not enhance, as discussed below.

In previous papers [24,28] we considered two reaction routes for thiophene HDS over the highly active supported Pt catalysts: (i) a monofunctional route in which HDS reaction proceeds only on Pt particles; and (ii) a bifunctional route in which both Pt particles and Brønsted acid sites are involved in HDS reactions. Because the Brønsted acidity of supports remarkably affected the HDS activity of supported Pt catalysts (Table 3), both Pt particles and Brønsted acid sites are important for highly active supported Pt catalyst. Furthermore, we found that the interaction between thiophene molecule and AlSBA-15 with Brønsted acid sites was stronger than those of SBA-15 and Na-AlSBA-15 without Brønsted acid sites (Fig. 10). Therefore, both Pt particles and Brønsted acid sites in Pt/AlSBA-15 catalyst also act as active sites in the HDS of thiophene as well as the HDS reaction over highly active Pt/Al_2O_3-modified silica gel (Al_2O_3-SiO_2) [28] and Pt/Al_2O_3-modified MCM-41 (Al_2O_3-MCM-41) [24] catalysts. Based on these results, we propose a possible mechanism of HDS reaction over highly active Pt/AlSBA-15 catalyst having Brønsted acid sites in which hydrogen is activated on Pt to form spillover hydrogen, and thiophene is activated on Brønsted acid sites of AlSBA-15, (Scheme 1). Some researchers reported that the C–S bond in thiophene molecules cleaves via thiophene-derived carbenium ions on Brønsted acid sites of zeolites [35–37]. Thiophene molecules adsorbed on Brønsted acid sites of AlSBA-15 are activated to form carbenium ions. The spillover hydrogen formed on Pt particles attacks the activated thiophene on the Brønsted acid sites of AlSBA-15. It was reported that migration of spillover hydrogen would be a rate-limiting step in the hydrogenation reaction [9]. Because the rate-limiting step in the HDS of thiophene over Pt/AlSBA-15 catalyst would also be migration of spillover hydrogen on the surface, HDS activity of Pt/AlSBA-15 was remarkably enhanced by increasing Pt loading (Fig. 11). Furthermore, the HDS activity of 5 wt%

Pt-loaded catalyst was the same as that of 7 wt% Pt-loaded catalyst, which can be explained by the saturation of spillover hydrogen on the catalyst surface when Pt loading was more than 5 wt%.

4. CONCLUSION

It was revealed that the Pt/AlSBA-15 catalyst showed high and stable activity for the HDS of thiophene, and that this activity was higher than that of commercial $CoMo/Al_2O_3$ HDS catalyst. The characterization results revealed that highly active Pt/AlSBA-15 catalyst showed high Pt dispersion and high Brønsted acidity. Furthermore, the interaction between thiophene molecules and AlSBA-15 with Brønsted acid sites was stronger than that of SBA-15 without Brønsted acid sites. These results indicate that both Pt particles and Brønsted acid sites in Pt/AlSBA-15 catalyst act as active sites in the HDS of thiophene.

References

[1] R. Prins, V.H.J. de Beer, G.A. Somorjai, Catal. Rev.-Sci. Eng. 31 (1989) 1-41.

[2] R.R. Chianelli, M. Daage, M.J. Ledoux, Adv. Catal. 40 (1994) 177-232.

[3] H. Topsøe, B.S. Clausen, F.E. Massoth, Catal. Sci. Tech. 11 (1996) 1−310.

[4] D.D. Whitehurst, T. Isoda, I. Mochida, Adv. Catal. 4 (1998) 345-471.

[5] M. Sugioka, PETROTECH 19 (6) (1996) 458-462.

[6] T. Kabe, A. Ishihara, W. Qian, Hydrodesulfurization and Hydrodenitrogenation, Kodansha Scientific, Wiley-VCH, Tokyo, New York, Berlin, 1999.

[7] J. Lee, A. Ishihara, F. Dumeignil, K. Miyazaki, Y. Oomori, E.W. Qian, T. Kabe, T., J. Mol. Catal. A 209 (2004) 155-162.

[8] R. Navarro, B. Pawelec, J.L.G. Fierro, P.T. Vasudevan, J.F. Cambra, M.B. Guemez, P.L. Arias, Fuel Process. Technol. 61 (1999) 73-88.

[9] X. Li, A. Wang, Z. Sun, C. Li, J. Ren, B. Zhao, Y. Wang, Y. Chan, Y. Hu, Appl. Catal. A 254 (2003) 319-326.

[10] Y. Yoshimura, H. Yasuda, T. Sato, N. Kijima, T. Kameoka, Appl. Catal. A 207 (2001) 303-307.

[11] V.L. Barrio, P.L. Arias, J.F. Cambra, M.B. Güemez, B. Pawelec, J.L.G. Fierro, Catal. Commun. 5, (2004) 173-178.

[12] M.A. Al-Saleh, M.M. Hossain, M.A. Shalabi, T. Kimura, T. Inui, Appl. Catal. A 253 (2003) 453-459.

[13] M. Sugioka, Erdöl und Kohle Erdgas Petrochemie 48 (1995) 128-132.

[14] M. Sugioka, F. Sado, T. Kurosaka, X. Wang, Catal. Today 45 (1998) 327-334.

[15] T. Kurosaka, M. Sugioka, H. Matsuhashi, Bull. Chem. Soc. Jpn. 74 (2001) 757-763.

[16] K.M. Reddy, B. Wei, C. Song, Catal. Today 43 (1998) 261-272.

[17] A. Wang, Y. Wang, T. Kabe, Y. Chen, A. Ishihara, W. Qian, J. Catal. 199 (2001) 19-29.

[18] A. Sampieri, S. Pronier, J. Blanchard, M Breysse, S. Brunet, K. Fajerwerg, C. Louis, G. Pérot, Catal. Today, 107-108 (2004) 537-544.

[19] T. Klimova, L. Lizama, J.C. Amezcua, P. Roquero, E. Terrés,J. Navarrete, J.M. Domínguez Catal. Today, 98 (2004) 141-150.

[20] M. Sugioka, L. Andalaluna, S. Morishita, T. Kurosaka, Catal. Today 39 (1997) 61-67.

[21] M. Sugioka, S. Morishita, T. Kurosaka, A. Seino, M. Nakagawa, S. Namba, Stud. Surf. Sci. Catal. 125 (1999) 531-538.

[22] M. Sugioka, T. Kurosaka, J. Jpn. Petrol. Inst. 45 (2002) 342-354.

[23] Y. Kanda, Y. Uemichi, T. Kobayashi, L. Andalaluna, M. Sugioka, Stud. Surf. Sci. Catal. 156 (2005) 747-754.

[24] Y. Kanda, T. Kobayashi, Y. Uemichi, S. Namba, M. Sugioka, Appl. Catal. A, 308 (2006) 111-118.

[25] J.H.A. Martens, R. Prins, Appl. Catal. 46 (1989) 31-44.

[26] B.Shelimov, J.F. Lambert, M. Che, B. Didillon, J. Catal., 185, (1999) 462-478.

[27] S. Boujday, J. Lehman, J.F. Lambert, M. Che, Catal. Lett. 88, (2003) 23-30.

[28] Y. Kanda, T. Kobayashi, Y. Uemichi, M. Sugioka, J. Jpn. Petrol. Inst. 49 (2006) 49-56.

[29] C. Song, X. Ma, Appl. Catal. B 41 (2003) 207-238.

[30] T.L. Tarbuck, K.R. McCrea, J.W. Logan, J.L.Heiser, M.E. Bussell, J. Phys. Chem. B 102 (1998) 7845-7857.

[31] P. Mills, D.C. Phillips, B.P. Woodruff, R. Main, M.E. Bussell, J. Phys. Chem. B 104 (2000) 3237-3249.

[32] F.T.T. Ng, A. Rahman, T. Ohasi, M. Jiang, Appl. Catal. B 56 (2005) 127-136.

[33] H. Soscún, O. Castellano, J. Hernázdez, J. Mol. Struct. 531 (2000) 315-321.

[34] X. Rozanska, R.A. van Santen, F. Hutschka, J. Hafner, J. Catal. 205 (2002) 388-397.

[35] H.H. Shan, C.Y. Li, C.H. Yang, H. Zhao, B.Y. Zhao, J.F. Zhang, Catal. Today 77 (2002) 117-126.

[36] A. Chica, K.G.. Strohmaier, E. Iglesia, Appl. Catal. B 60 (2005) 223-232.

[37] J.A. Valla, A.A. Lappas, I.A. Vasalos, Appl. Catal. A 297 (2006) 90-101.

[38] D. Zhao, J. Feng, Q. Huo, N. Melosh, G.H. Fredrickson, B.F. Chmelka and G.D. Stucky, Science 279 (1998) 548-552.

[39] S.K. Jana, R. Nishida, K. Shindo, T. Kugita, S. Namba, Microporous Mesoporous Mater. 68 (2004) 133-142.

Figure captions

Fig. 1. XRD patterns of (a) SBA-15 and (b) AlSBA-15.

Fig. 2. Nitrogen adsorption isotherm of (●) SBA-15 and (▲) AlSBA-15.

Fig. 3. Pore size distribution of (●) SBA-15 and (▲) AlSBA-15 calculated by nitrogen adsorption isotherm.

Fig. 4. Hydrodesulfurization of thiophene over noble metal/SBA-15 catalyst at 350 °C. (●) Pt; (▲) Pd; (■) Rh; (♦) Ru.

Fig. 5. Hydrodesulfurization of thiophene over noble metal/AlSBA-15 catalyst at 350 °C. (●) Pt; (▲) Pd; (■) Rh; (♦) Ru.

Fig. 6. Catalytic activities of Pt/HZSM-5[15], Pt/Al_2O_3-MCM-41[24], and Pt/AlSBA-15 for the HDS of thiophene at 350 °C.

Fig. 7. XRD patterns of platinum supported on (a) SBA-15 and (b) AlSBA-15.

Fig. 8. Catalytic activities of SBA-15 and AlSBA-15 for the (□) dehydration of 2-propanol (200 °C) and (■) cracking of cumene (400 °C).

Fig. 9. FT-IR spectra of pyridine adsorbed on (a) SBA-15 and (b) AlSBA-15. Pyridine was adsorbed at 150 ºC followed by evacuation at 150 °C for 0.5 h.

Fig. 10. FT-IR spectra of thiophene adsorbed on (a) SBA-15, (b) AlSBA-15, (c) 2 wt% Na-AlSBA-15, and (d) 4 wt% Na-AlSBA-15. (i) Samples evacuated at 500 °C for 2 h, (ii) thiophene (2 kPa) introduced, (iii) after evacuation at 25 °C for 0.5 h.

Fig. 11. Relation between Pt loading and HDS activity of Pt/AlSBA-15 catalyst at 350 °C.

Scheme 1 Possible mechanism of HDS of thiophene over highly active Pt/AlSBA-15 catalyst with Brønsted acid sites.

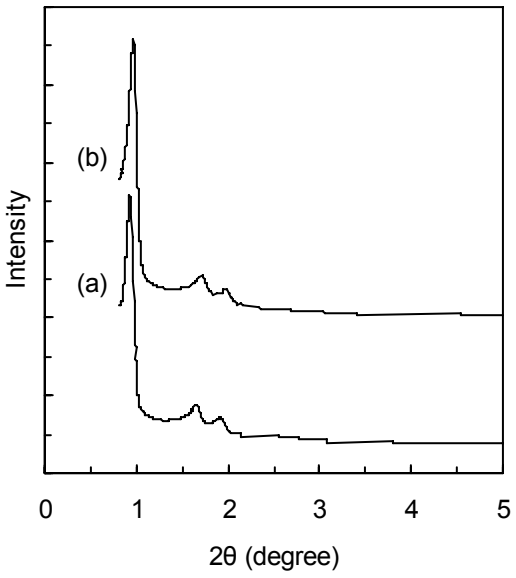

Fig. 1

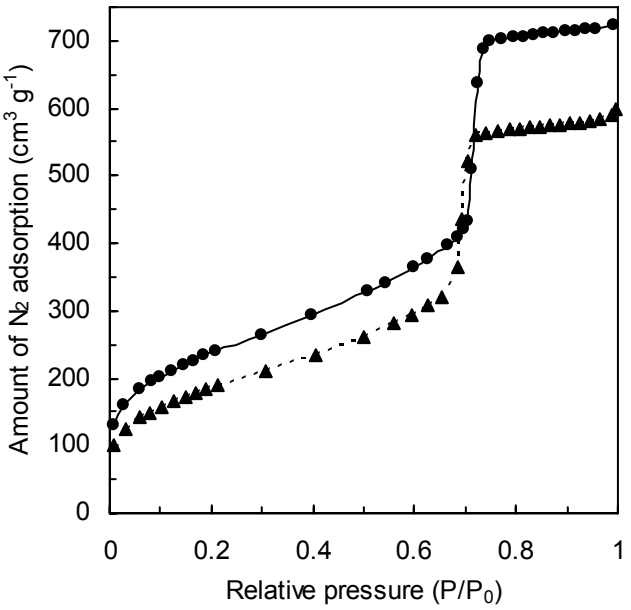
Amount of N2 adsorption (cm3 g-1)
700
600
500
400
300
200
100
0
0
0.2
0.4
0.6
0.8
1
Relative pressure (P/P0)

Fig. 2

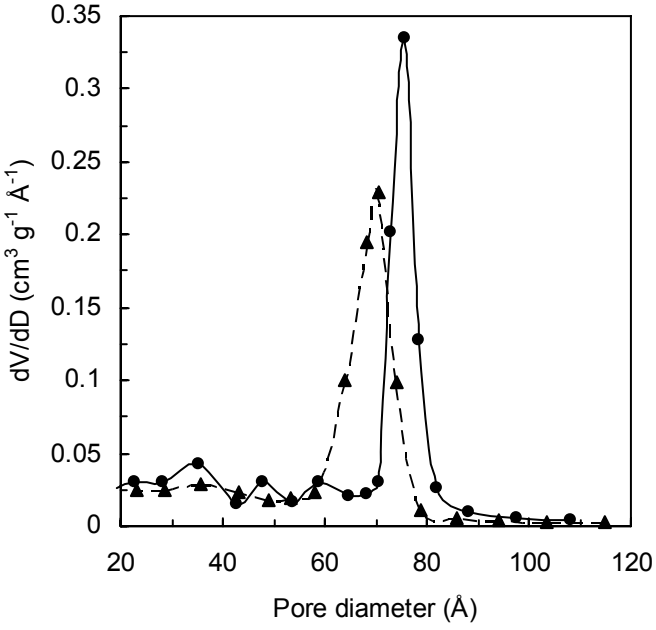
0.35
0.3
0.25
0.2
0.15
0.1
0.05
0
dV/dD (cm3 g-1 Å-1)
20
40
60
80
100
120
Pore diameter (Å)

Fig. 3

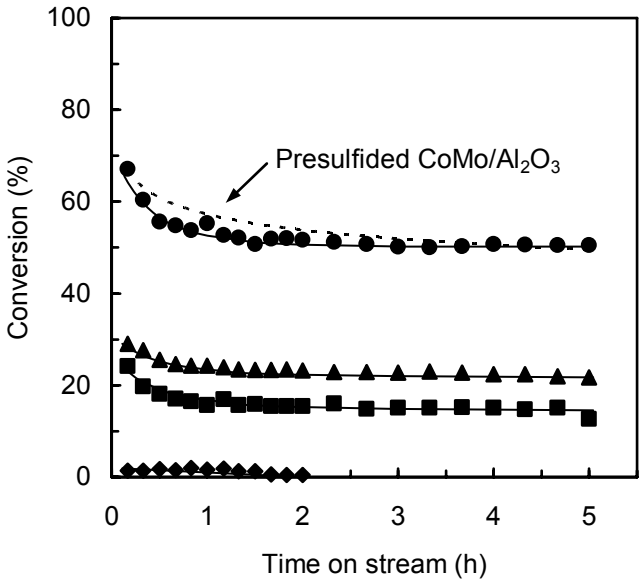

H_2/thiophene = 30, W/F = 37.9 g h mol^{-1}

Fig. 4

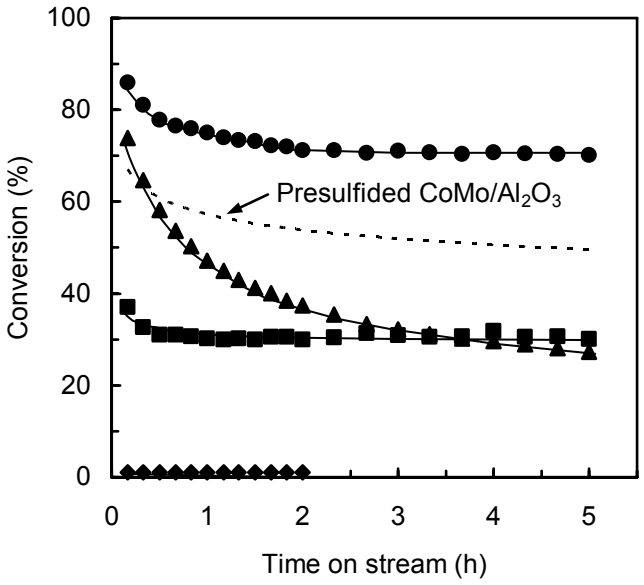

H_2/thiophene = 30, W/F = 37.9 g h mol^{-1}

Fig. 5

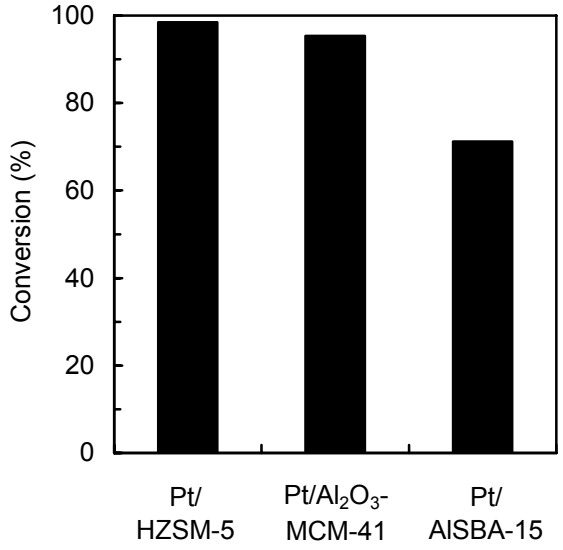
100
80
60
40
20
0
Conversion (%)
Pt/
HZSM-5
Pt/Al2O3-
MCM-41
Pt/
AlSBA-15

Fig. 6

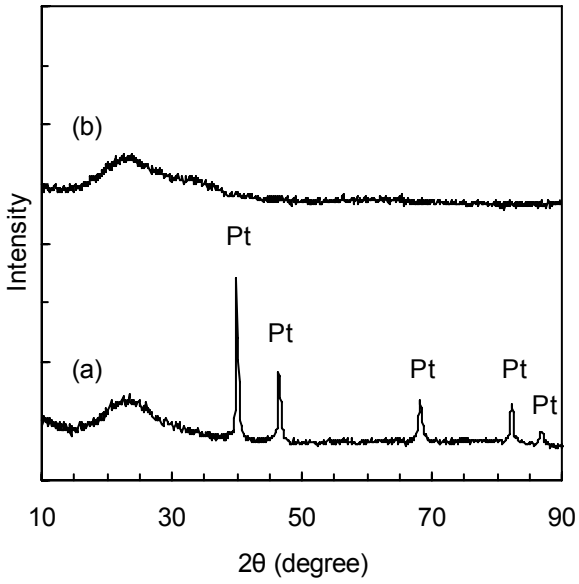

Fig. 7

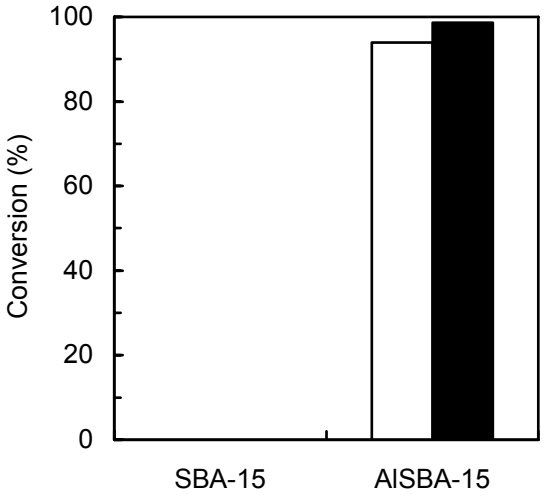

Fig. 8

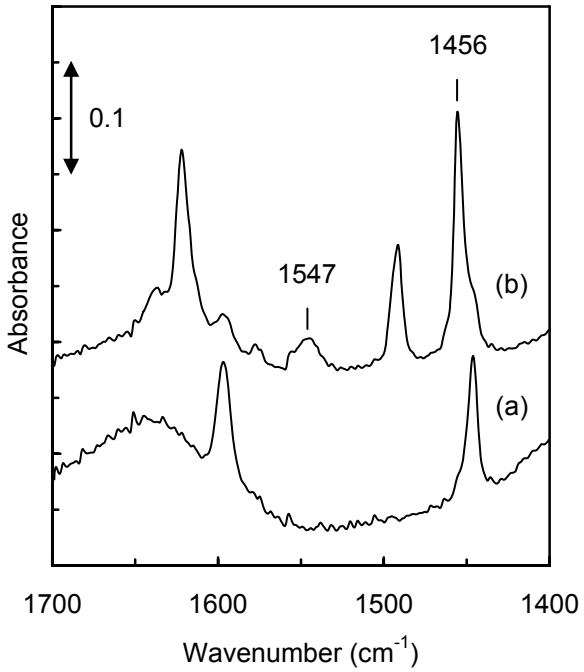
1456
0.1
1547
(b)
(a)
Absorbance
1700
1600
1500
1400
Wavenumber (cm-1)

Fig. 9

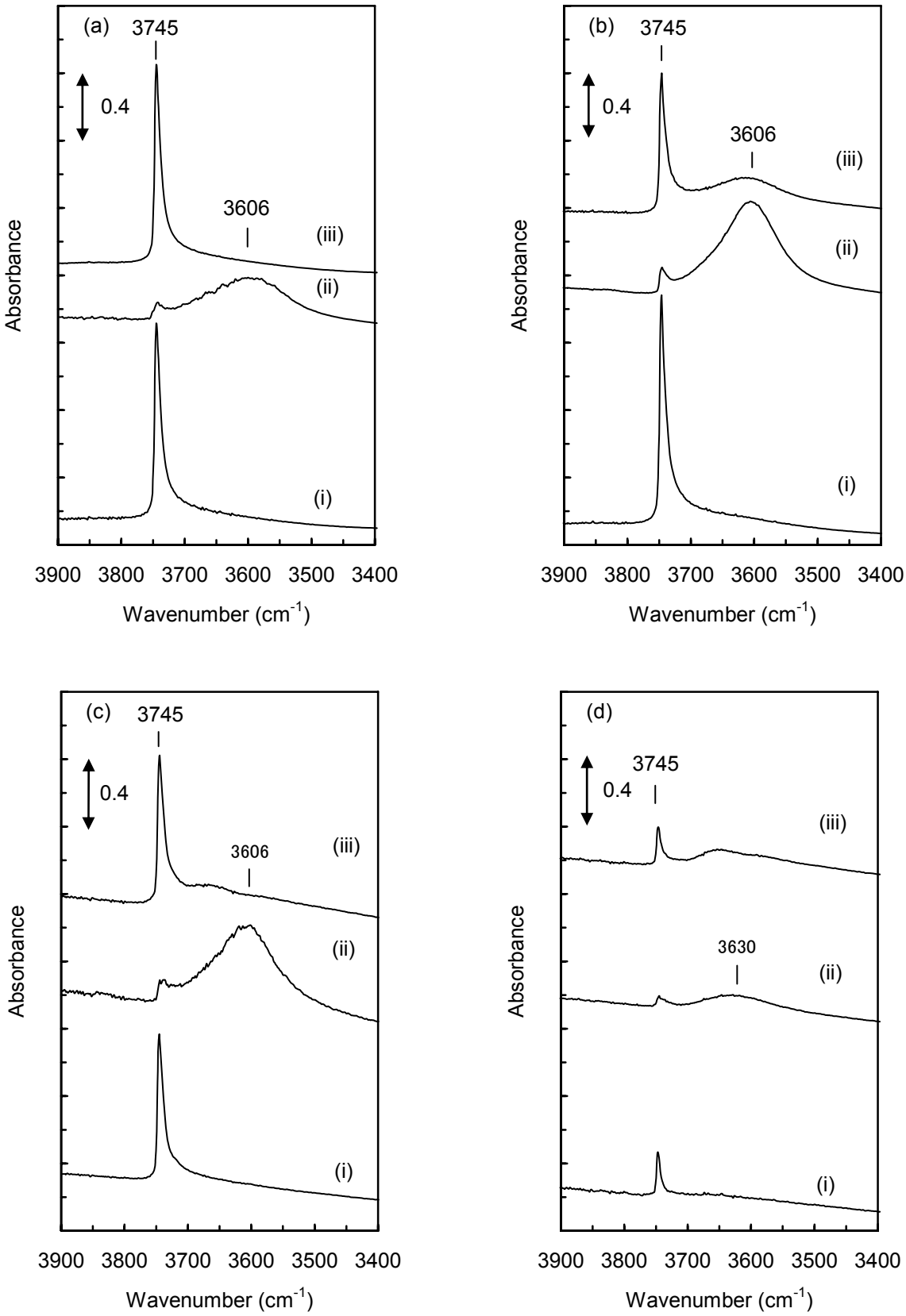
(a)
3745
0.4
3606
(iii)
(ii)
(i)
Absorbance
3900 3800 3700 3600 3500 3400
Wavenumber (cm-1)
(b)
3745
0.4
3606
(iii)
(ii)
(i)
Absorbance
3900 3800 3700 3600 3500 3400
Wavenumber (cm-1)
(c)
3745
0.4
3606
(iii)
(ii)
(i)
Absorbance
3900 3800 3700 3600 3500 3400
Wavenumber (cm-1)
(d)
3745
0.4
(iii)
3630
(ii)
(i)
Absorbance
3900 3800 3700 3600 3500 3400
Wavenumber (cm-1)

Fig. 10

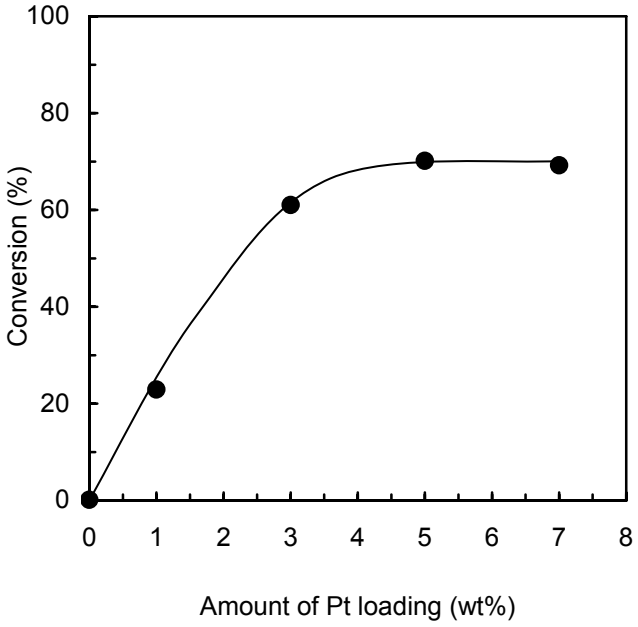
100
80
60
40
20
0
Conversion (%)
0
1
2
3
4
5
6
7
8
Amount of Pt loading (wt%)

Fig. 11

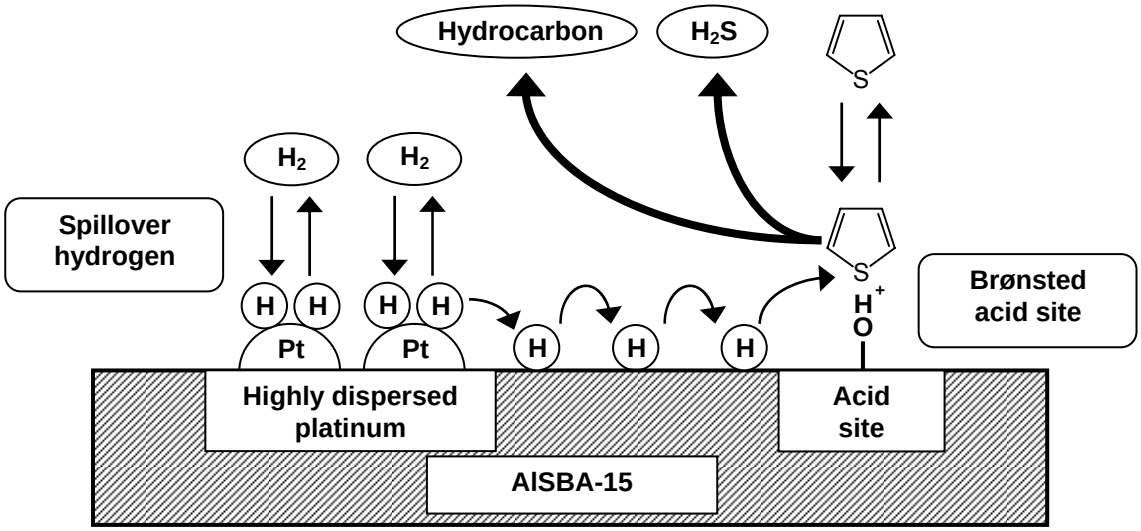
Hydrocarbon
H2S
S
H2
H2
Spillover hydrogen
S
H+
O
Brønsted acid site
H
H
H
H
H
H
H
Pt
Pt
Highly dispersed platinum
Acid site
AlSBA-15

Scheme 1

Table 1

Textural properties of SBA-15 and AlSBA-15 measured by nitrogen adsorption isotherm

Support	Surface area ($m^2\ g^{-1}$)	Pore volume ($cm^3\ g^{-1}$)
SBA-15	847	1.12
AlSBA-15	666	0.91

Table 2

Dispersion and particle size of Pt on SBA-15 and AlSBA-15

Catalyst	Dispersion of Pt (H/Pt)	Particle size (nm)	
		H_2 adsorption	XRD*
Pt/SBA-15	0.53	1.79	14.4
Pt/AlSBA-15	0.77	1.23	-

* Calculated by Scherrer equation.

Table 3

Effect of sodium addition on HDS activity and catalytic properties of Pt/AlSBA-15

Na content (wt %)	HDS (%)	Pt dispersion (H/Pt)	Cumene cracking[a)] (%)	2-PA dehydration[a)] (%)
0	74.4	0.77	98.7	100
0.5	65.5	0.75	50.9	88.9
1.0	41.0	0.71	18.1	66.1
2.0	28.5	0.78	0.3	3.4
4.0	6.2	0.14	0.0	0.0

a) Activities of supports (0.03 g)